Research article

Effects of MCI-186 upon neutrophil-derived active oxygens

K. Sumitomo[1,2], N. Shishido[3], H. Aizawa[2], N. Hasebe[2], K. Kikuchi[2], M. Nakamura[3]

[1]Nakatombetsu National Health Insurance Hospital, Nakatombetsu, Japan
Departments of [2]Internal Medicine and [3]Chemistry, Asahikawa Medical College, Asahikawa, Japan

Reactions of 3-methyl-1-phenyl-2-pyrazoline-5-one (MCI-186) with hypochlorous acid and superoxide were analysed by spectrophotometry and mass spectrometry. The results were applied to the neutrophil system to evaluate the scavenging activity of neutrophil-derived active oxygen species by MCI-186. MCI-186 reacted rapidly with hypochlorous acid (1×10^6 $M^{-1}s^{-1}$) to form a chlorinated intermediate, followed by a slow conversion to a new spectrum. MCI-186 consumed 3 moles of hypochlorous acid and did not react with superoxide. The newly synthesized fluorescence probes, 2-[6-(4′-amino)phenoxy-3H-xanthen-3-on-9-yl]benzoic acid (APF) and 2-[6-(4′-hydroxy)-phenoxy-3H-anthen-3-on-9-yl]benzoic acid (HPF) successfully detected neutrophil-derived active oxygens (Setsukinai K, Urano Y, Kakinuma K, Majima HJ, Nagano T. Development of novel fluorescence probes that can reliably detect reactive oxygen species and distinguish specific species. *J Biol Chem* 2003; **278:** 3170–3175). The rate constants for the reaction of hypochlorous acid with MCI-186 and fluorescence probes was in the order of MCI-186 > APF > HPF. Fluorescence due to the oxidation of APF and HPF was observed with the stimulated neutrophils. The result that the intensity from APF oxidation was higher than that from HPF oxidation is compatible with reports that APF selectively reacts with hypochlorous acid. Fluorescence due to oxidation of both APF and HPF decreased when the reactions were carried out in the presence of a fluorescence probe and MCI-186 in a dose-dependent manner. These results indicate that MCI-186 effectively scavenges neutrophil-derived hypochlorous acid and other active oxygens.

Keywords: MCI-186, neutrophil-derived active oxygens, APF, HPF

INTRODUCTION

It is known that phagocytosing neutrophils induce a burst of oxygen consumption catalyzed by an assembled NADPH oxidase, generating superoxide.[1,2] Superoxide undergoes a dismutation reaction by superoxide dismutase (SOD) to produce H_2O_2 and oxygen. It has been estimated that 25–70% of the generated H_2O_2 is utilized for HOCl formation by the action of myeloperoxidase. Hypochlorous acid plays an important role in the bactericidal action of neutrophils.[2–5]

Received 29 January 2007
Revised 1 May 2007
Accepted 16 May 2007

Correspondence to: Masao Nakamura PhD, Department of Chemistry, Asahikawa Medical College, Midorigaokahigashi 2-1-1-1, Asahikawa 078-8510, Hokkaido, Japan
Tel: +81 166 68 2724; Fax: +81 1 66 68 2782;
E-mail: nmasao@asahikawa-med.ac.jp

Much attention has been paid to the other oxidant, the hydroxyl radical (HO•), since biomarkers of oxidative stress in the cells are formed through the reactions of hydroxyl radicals with biomolecules.[6,7] Redox properties of hydroxyl radicals are well documented. Hydroxyl radicals are formed through the Fenton-type Haber Weiss reaction and through the reaction of superoxide with hypochlorous acid.

Fluorescence probes, 2′,7′-dichlorodihydrofluorescein and dihydrorhodamine 123, are used for the detection of active oxygen species *in vivo*, although both probes are auto-oxidizable and have no specificity for oxidants. The newly synthesized fluorescence probes, 2-[6-(4′-amino)-phenoxy-3H-xanthen-3-on-9-yl]benzoic acid (APF) and 2-[6-(4′-hydroxy)phenoxy-3H-xanthen-3-on-9-yl]-benzoic acid (HPF) react with the active oxygens, hydroxyl radicals and peroxynitrite.[8,9] It is important to note that APF reacts with hypochlorous acid, but HPF almost never does. Setsukinai *et al.*[8] confirmed that

DOI 10.1179/135100007X200317

APF-loaded neutrophils show a marked increase in fluorescence after stimulation.

The free radical scavenger, 3-methyl-1-phenyl-2-pyrazoline-5-one (MCI-186), has been shown to attenuate ischemia and post ischemic brain edema induced by the middle cerebral artery occlusion model in rats.[10,11] The clinical efficacy of MCI-186 has been attributed to the scavenging ability of hydroxyl and lipid peroxy radicals.[12–14] We observed that MCI-186 reacted rapidly with hypochlorous acid. This article determines the contribution of MCI-186 to the scavenging activity of neutorophil-derived active oxygens.

Materials and Methods

3-Methyl-1-phenyl-2-pyrazoline-5-one (MCI-186) was provided by Mitsubishi Pharma Co. (Osaka, Japan). Myeloperoxidase (MPO) from human leukocytes, cytochrome c from horse hearts, xanthine oxidase from bovine milk, xanthine and GSH, monochlorodimedone (MCD), SOD from bovine erythrocytes, catalase from bovine liver and phorbol myristate acetate (PMA) were purchased from Sigma-Aldrich Japan (Tokyo, Japan). Sodium hypochlorite solution (NaOCl) and luminol were obtained from Wako Pure Chemical Industry (Osaka, Japan).

2-[6-(4′-amino)phenoxy-3H-xanthen-3-on-9-yl]-benzoic acid (APF) and 2-[6-(4′-hydroxy)phenoxy-3H-xanthen-3-on-9-yl]benzoic acid (HPF) were purchased from Daiichi Pure Chemicals Co., Ltd (Japan).

Reactions were carried out at 25°C in 40 mM phosphate (pH 7.4) unless otherwise stated.

Spectrophotometric measurements were performed with a Shimadzu MPS-2000 spectrophotometer. Desorption chemical ionization (DCI) mass spectrometry was performed with a JEOL JMS-SX102QQ.

Reaction of MCI-186 with superoxide and HOCl

Superoxide was generated by the xanthine oxidase system and detected by the reduction of cytochrome *c*, which followed an increase in absorbance at 550 nm.[15] Reaction of MCI-186 with superoxide was analyzed by the inhibitory effect of MCI-186 upon the cytochrome *c* reduction by the xanthine oxidase system. The concentration of HOCl was determined by the reaction of HOCl with MCD. The concentration of HOCl in the mixtures was calculated from the mole absorption coefficient of monochlorodimedone at 290 nm.[16,17] Based on the rate constant for the reaction of HOCl with MCD, the rate constant for the reaction of MCI-186 with HOCl was calculated.

Reaction of APF and HPF with superoxide and HOCl

Reaction of superoxide with APF and HPF was analyzed by the inhibitory effect of fluorescent probes upon the cytochrome *c* reduction by xanthine oxidase system. Oxidation of APF and HPF with HOCl was followed as an increase in absorbance at 510 nm.

Detection of active oxygen species in neutrophils

Neutrophils suspension was prepared as follows.[14] Venous peripheral blood from healthy volunteers was incubated in NH_4Cl (8.26 g/l), $KHCO_3$ (1.0 g/l) and ethylenediaminetetraacetic acid tetrasodium salt (0.037 g/l) in Chelex-100 treated water (pH 7.3) for 10 min to lyse erythrocytes, washed with ice-cold 2-[4-(2-hydroxyethyl)-1-piperazinyl] ethanesulfonic acid (HEPES) buffer and then centrifuged at 1000 *g* at 4°C for 5 min. The supernatant was discarded. Neutrophils were resuspended in 1 ml HEPES buffer.

To measure intracellular reactive oxygen species of neutrophils, neutrophils were pre-incubated at 37°C for 15 min in HEPES buffer (pH 7.4) in the presence of 2 μM APF or HPF. The reactions were started by the addition of 100 nM PMA and incubated for 10 min, then the 5 μl portion of each reaction mixture was subjected to flow cytometry (EPICS XL/XL-MCL system II v.3.0, Becton Dickinson). Data are shown as mean fluorescence intensity for 5 x 10^3 cells.

To measure extracellular superoxide generation by neutrophils, neutrophils (2 x 10^5 cells) were stimulated with 100 nM PMA in the presence of 10 μM luminol. Chemiluminescence of luminol through the reaction of luminol with superoxide was detected with a luminometer (BLR-301, ALOKA, Japan).

Results and Discussion

The antioxidant activity of MCI-186 is ascribed to the radical scavenging activity of the pyrazoline 5-one moiety of MCI-186.[12,13,18–20] Using pulse radiolysis, it has been reported that pyrazole itself does not react with $Br_2^{\cdot-}$ radicals, whereas pyrazoline 5-one does.[18] Pyrazole is a fully aromatic molecule, while the pyrazoline 5-one ring is partially saturated. The results suggest that pyrazoline 5-one could scavenge oxidative radicals. MCI-186 was found to inhibit lipid peroxidation in liposomal membranes.[12] Lipid peroxidation is explained in terms of the chain reaction, involving the formation of carbon-centered radicals and lipidperoxy radicals. MCI-186 should react with lipidperoxy radicals to inhibit the chain reaction. In this experiment, lipid peroxidation was initiated by the thermal decomposition

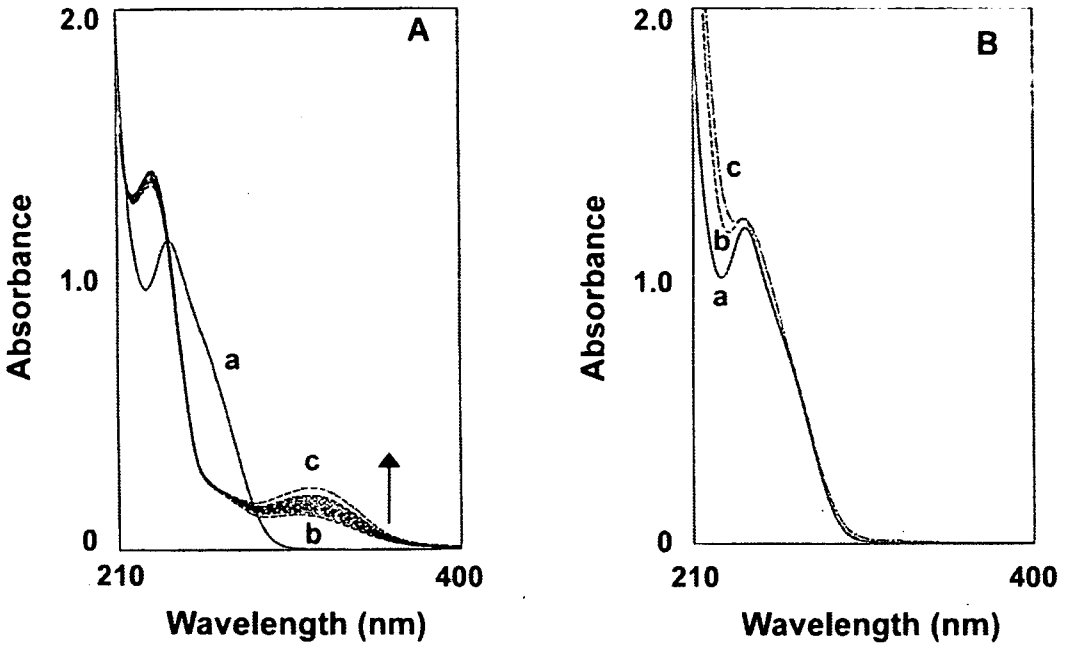

Fig. 1. Spectral changes of MCI-186 by the addition of HOCl in the absence (A) or presence (B) of GSH. (A) The spectrum of MCI-186 (a) changed immediately to spectrum (b) by the addition of HOCl. The spectrum was recorded at intervals of 10 min. Spectrum (c) was obtained at 120 min after the addition of HOCl. The reaction mixture contained 100 μM MCI-186 and 200 μM HOCl in 40 mM phosphate buffer (pH 7.4). Similar spectral changes were observed when 100 μM MCI-186 was treated with myeloperoxidase system (0.25 units MPO/100 μM H_2O_2/10 mM KCl). (B) Spectrum (c) was obtained by the addition of 200 μM HOCl to the reaction mixture (spectrum b) which contained 100 μM MCI-186 and 200 μM GSH in 40 mM phosphate buffer (pH 7.4).

of azo compounds under aerobic conditions. It is important to note that MCI-186 reduces the lipid peroxidation started by the water- and lipid-soluble initiator. These results indicate that MCI-186 is located on the surface and/or near the lipid membrane, because MCI-186 has a lipophilic moiety.

Neutrophils produce superoxide-derived active oxygen species, hydroxyl radicals, hypochlorous acid and peroxynitrite.[2,3,21] Superoxide was generated by the xanthine oxidase system and detected by the reduction of cytochrome *c*. The generation of superoxide by the xanthine oxidase system proceeded at a rate of 2.5 μM/min. The reduction of cytochrome *c* was completely diminished in the presence of 0.1 μM SOD and 0.08 μM catalase. No effect of 200 μM MCI-186 upon the initial velocity of the reduction of cytochrome *c* was observed. Superoxide was also detected by chemiluminescence of luminol using a luminometer. Chemiluminescence of luminol by the xanthine oxidase system was not inhibited in the presence of 100 μM MCI-186. No reaction of superoxide with MCI-186 has been suggested.

It has been reported that MCI-186 reacts with hydroxyl radicals. Using spin trap DMPO, the rate constant for the reaction of MCI-186 with hydroxyl radical is estimated to be 3.0×10^{10} $M^{-1}s^{-1}$.[20]

Reaction of MCI-186 with HOCl was followed optically in the UV region (Fig. 1A). Spectrum (a), MCI-186, which has an absorption peak at 237 nm, was converted to spectrum (b) by the addition of HOCl. Spectrum (b) appeared within the mixing time, and was followed by a slow conversion to spectrum (c) (Fig. 1A). Spectral changes of MCI-186 to spectrum (c) (Fig. 1A) were abolished when the reaction was started in the presence of an equimolar concentration of GSH to MCI-186 (Fig. 1B). Spectrum (b) in Figure 1A returned to the initial spectrum by the addition of GSH (data not shown). Thiols (Cys, GSH) should remove chlorine from chloramines. Spectrum (b) was also obtained with the myeloperoxidase system ($MPO/H_2O_2/Cl^-$). These results indicate that spectrum (b) in Figure 1A is a chlorinated compound. The rate constant for the reaction of MCI-186 with HOCl was estimated to be 7×10^6 $M^{-1}s^{-1}$ from the competition kinetics.

Table 1. Reaction of HOCl with reactants

Compounds	Rate constants* ($M^{-1}s^{-1}$)
MCI-186	7×10^6
APF	2×10^5
HPF	$< 10^2$
GSH	$> 10^7$

*Rate constants were estimated from the competition kinetics.[16,17]

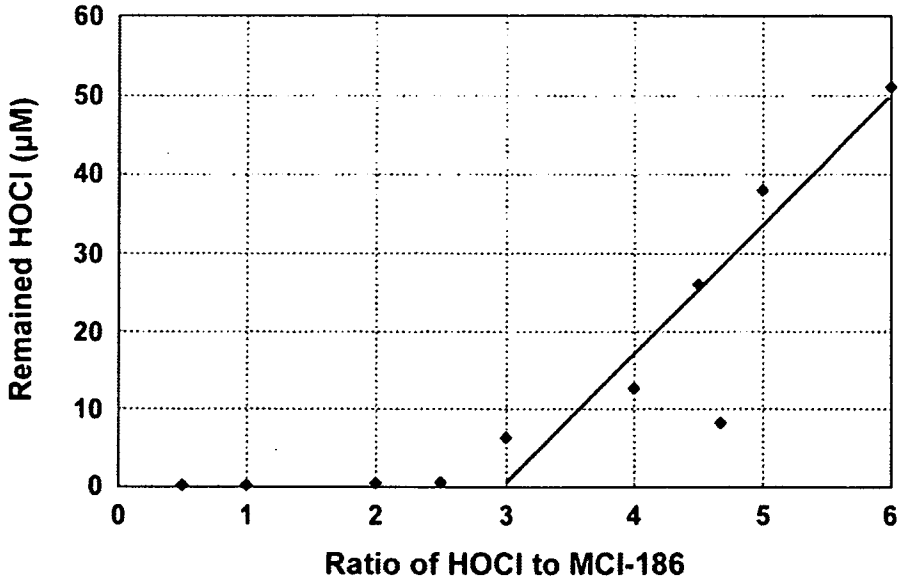

Fig. 2. Concentrations of HOCl after reaction with MCI-186. The reaction mixtures contained 50 μM MCI-186 and various concentrations of HOCl. After 30 min, the remaining concentration of HOCl was determined by reaction with MCD.

This rate constant is slightly slower than that for the reaction of GSH with HOCl (Table 1).

After reaction of MCI-186 with HOCl, the remaining concentration of HOCl was detected by a decrease in absorbance at 290 nm. From the molar absorption coefficient of monochlorodimedone, the concentration of HOCl remaining in the mixtures was calculated (Fig. 2). The results indicated that MCI-186 consumed 3 moles of HOCl per mole MCI-186.

The reaction mechanism of MCI-186 with lipidperoxy radicals, which leads to the final oxidation product, has been documented.[12] One-electron oxidation of MCI-186

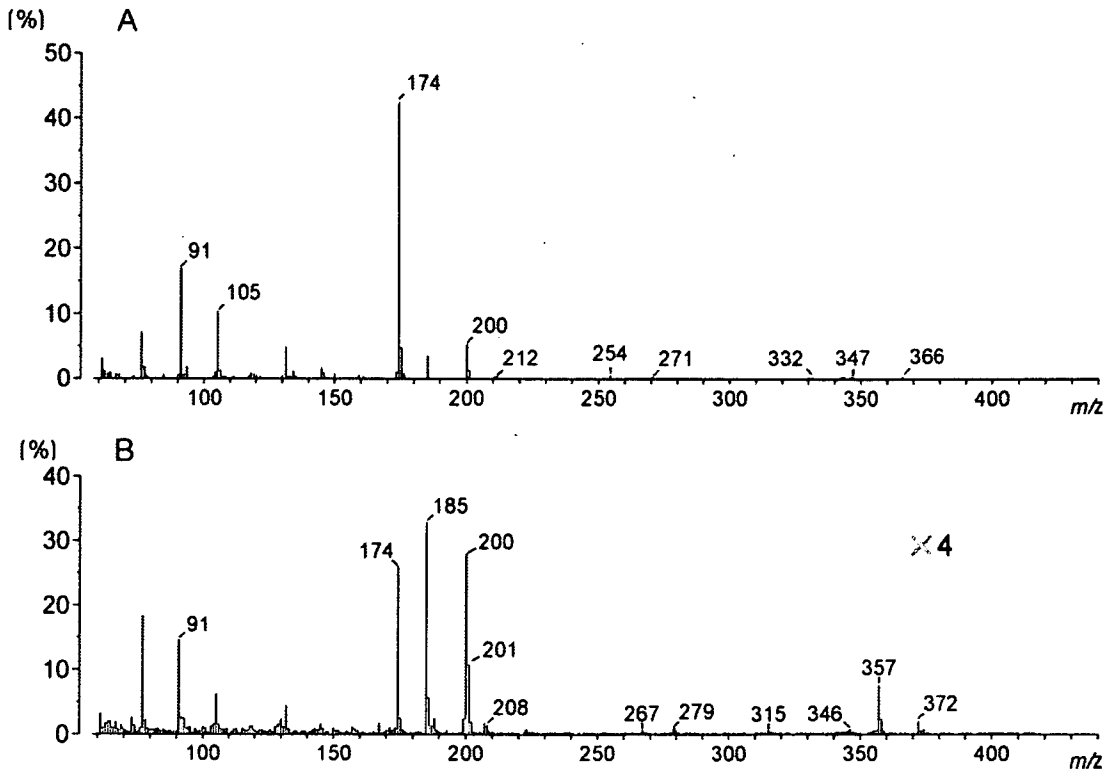

Fig. 3. Mass spectra of MCI-186 in the absence (A) or presence (B) of HOCl. The reaction mixture contained 200 μM MCI-186 and was incubated for 30 min in the absence (A) or presence (B) of 600 μM HOCl. Aliquots of the reaction mixture were applied for DCI mass spectrometry.

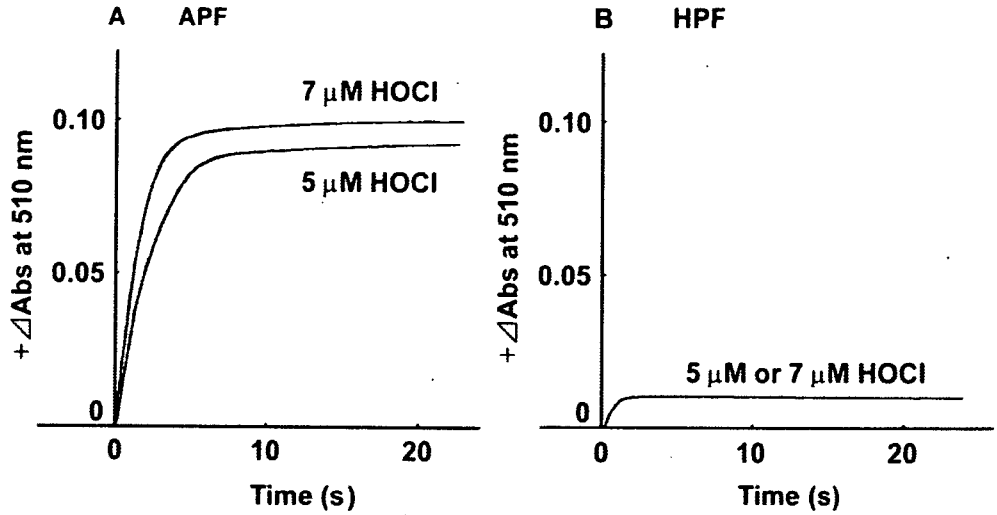

Fig. 4. Time course for the reaction of APF (A) and HPF (B) with HOCl. The reaction mixtures contained 1 μM APF (A) or HPF (B) and various concentrations of HOCl. Reactions were started by the addition of HOCl.

results in the formation of MCI-186 radicals and initiates the formation of 2-oxo-3-(phenylhydrazono)-butanoic acid (OPB) through the transient formation of 3-methyl-1-phenyl-2-pyrazoline-4,5-dione (4,5-dione). In this reaction, the stoichiometric amount of OPB is formed. One-electron oxidation of MCI-186 with hydroxyl radicals initiates the same reaction mechanism, giving the formation of OPB.[20] The final reaction products of MCI-186 after reaction with HOCl were analyzed by DCI mass spectrometry. Figure 3A shows a mass spectrum of MCI-186, which gave the expected signal at 174 *m/z* and fragmented peaks (132, 105, 91 *m/z*). The MCI-186 peak was decreased with an increasing concentration of HOCl. The reaction mixture after the reaction of 0.2 mM MCI-186 with 4-fold molar excess of HOCl was subjected to mass spectrometry. Trace amounts of a new compound (357 *m/z*) were detected but neither OPB (206 *m/z*) nor 4,5-dione (189 *m/z*) was found (Fig. 3B). Decomposition of MCI-186 was inhibited when MCI-186 was treated with HOCl in the presence of equimolar concentrations of GSH to HOCl. There is no conclusive evidence, but the chlorinated MCI-186 seems to have been decomposed in a different manner.[12,20]

Newly developed fluorescence probes, APF and HPF, were used to detect active oxygen species in neutrophils. The ratio of APF to HPF fluorescence intensity after the reaction with HOCl was 3600 to 6.[8] Oxidation of both APF and HPF was followed optically at 510 nm (Fig. 4),

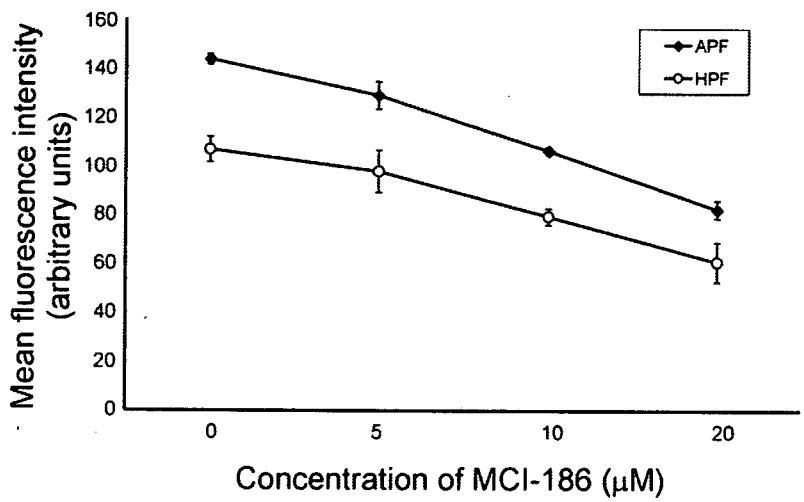

Fig. 5. Effect of MCI-186 concentration upon the fluorescence intensity of APF or HPF-loaded neutrophils. Neutrophils (1 x 10^6 cells/ml) from healthy volunteers were pre-incubated at 37°C for 15 min in HEPES buffer in the presence of both a 2 μM fluorescence probe and various concentrations of MCI-186. The neutrophils were stimulated with 100 nM PMA and incubated for 10 min, then 5 μl aliquots of the reaction mixture were subjected to flow cytometry. Data are shown as mean fluorescence intensity for 5 x 10^3 cells.

because the oxidation mechanism of APF and HPF with active oxygens has been previously documented[8,9] and both oxidation products have a new absorption at 510 nm. When both fluorescence probes were treated with xanthine oxidase system or 200 μM H_2O_2, no increase in absorbance at 510 nm was observed. We have confirmed no reaction of APF and HPF with superoxide or H_2O_2. At fixed concentrations of APF and HPF, the oxidation rate of APF was increased with an increasing concentration of HOCl (Fig. 4A). The rate constant for the reaction of APF with HOCl is estimated to be 1×10^5 $M^{-1}s^{-1}$ from kinetic traces. On the contrary, an increase in absorbance at 510 nm was only observed to a limited extent in the reaction of HPF with HOCl (Fig. 4B). The kinetic results support the hypothesis that APF reacts selectively with HOCl.[8]

APF or HPF was loaded into neutrophils. The fluorescent probe-loaded neutrophils were incubated for 15 min at 37°C and stimulated with 100 nM PMA. Both fluorescent probes were effectively oxidized and there was a significant difference in the intensity of fluorescence in the APF- and HPF-loaded neutrophils (Fig. 5). The results are compatible with the observation that APF reacts selectively with HOCl.[8] When the neutrophils were incubated in the presence of both a fluorescence probe and MCI-186, the fluorescence intensity after stimulation decreased with the increasing concentrations of MCI-186 (Fig. 5). Effective reduction in the fluorescence intensity was found in APF-loaded neutrophils. No effect of 10 μM MCI-186 upon the chemiluminescence of luminol by activated neutrophils was observed (data not shown). The result was in agreement with the observation that MCI-186 did not react with superoxide. This result indicates that MCI-186 scavenges most intracellular reactive oxygen species except superoxide. Both fluorescence probes have been observed to react rapidly with hydroxyl radicals and peroxynitrite.[8,20] NO synthase and myeloperoxidase are present in neutrophils. The present results indicate that MCI-186 competes with fluorescence probes for the reaction with neutrophils-derived active oxygens. It has been suggested that MCI-186 is located on the surface and/or near the membrane of cells where it can scavenge oxidative species.[12] The effect of MCI-186 on active oxygen scavenging activity is restricted to the spatial distribution of MCI-186.

ACKNOWLEDGEMENTS

We thank Mr Hiroaki Akutsu for the mass spectrometry studies (Central Laboratory for Research and Education) and Ms Sharon Hanley for critical reading of the manuscript.

REFERENCES

1. Segal AW, Abo A. The biochemical basis of the NADPH oxidase of phagocytes. *Trends Biochem Sci* 1993; **18**: 43–47.
2. Hampton MB, Kettle AJ, Winterbourn CC. Inside the neutrophile phagosome: oxidants, myeloperoxidase, and bacterial killing. *Blood* 1998; **92**: 3007–3017.
3. Foote CS, Goyne TE, Lehrer RI. Assessment of chlorination by human neutrophils. *Nature* 1983; **301**: 715–716.
4. Klebanoff SJ. Myeloperoxidase: occurrence and biological function. In: Grisham MB, Everse J. (eds) *Peroxidases in Chemistry and Biology*, vol. 1. Boca Raton, FL: CRC Press, 1991; 1–35.
5. Shishido N, Nakamura S, Nakamura M. Dissociation of DNA double strand by hypohalous acids. *Redox Report* 2000; **5**: 243–247.
6. Halliwell B, Gutteridge JM. Oxygen free radicals and iron in relation to biology and medicine: some problems and concepts. *Arch Biochem Biophys* 1986; **246**: 501–514.
7. Candeias LP, Patel KB, Stratford MR, Wardman P. Free hydroxyl radicals are formed on reaction between the neutrophil-derived species superoxide anion and hypochlorous acid. *FEBS Lett* 1993; **333**: 151–153.
8. Setsukinai K, Urano Y, Kakinuma K, Majima HJ, Nagano T. Development of novel fluorescence probes that can reliably detect reactive oxygen species and distinguish specific species. *J Biol Chem* 2003; **278**: 3170–3175.
9. Tomizawa S, Imai H, Tsukada S *et al.* The detection and quantification of highly reactive oxygen species using the novel HPF fluorescence probe in a rat model of focal cerebral ischemia. *Neurosci Res* 2005; **53**: 304–313.
10. Abe K, Yuki S, Kogure K. Strong attenuation of ischemic and postischemic brain edema in rats by a novel free radical scavenger. *Stroke* 1988; **19**: 480–485.
11. Nishi H, Watanabe T, Sakurai H, Yuki S, Ishibashi A. Effect of MCI-186 of brain edema in rats. *Stroke* 1989; **20**: 1236–1240.
12. Yamamoto Y, Kuwahara T, Watanabe K, Watanabe K. Antioxidant activity of 3-methyl-1-phenyl-2-pyrazolin-5-one. *Redox Report* 1996; **2**: 333–338.
13. Watanabe K, Watanabe K, Kuwahara T, Yamamoto Y. Free radical-induced oxidation products of 3-methyl-1-phenyl-2-pyrazolin-5-one (MCI-186). *Nihon yukagaku kaishi* (Japan Oil Chemists' Society, Tokyo) 1997; **46**: 797–801.
14. Aizawa H, Makita Y, Sumitomo K *et al.* Edaravone diminishes free radicals from circulating neutrophils in patients with ischemic brain attack. *Intern Med* 2006; **45**: 1–4.
15. Nakamura M, Kurebayashi H, Yamazaki Y. One-electron and two-electron reductions of acceptors by xanthine oxidase and xanthine dehydrogenase. *J Biochem* 1978; **83**: 9–17.
16. Kettle AJ, Winterbourn CC. The mechanism of myeloperoxidase-dependent chlorination of monochlorodimedone. *Biochim Biophys Acta* 1988; **957**: 185–191.
17. Folkes LK, Candeias LP, Wardman P. Kinetics and mechanisms of hypochlorous acid reactions. *Arch Biochem Biophys* 1995; **323**: 120–126.
18. Jovanovic SV, Neta P, Simic MG. One-electron reactions of pyrazolin-5-ones. A pulse radiolysis study of antipyrine and analogues. *Mol Pharmacol* 1985; **28**: 377–380.
19. Lehmann FM, Bretz N, von Bruchhausen F, Wurm G. Substrates for arachidonic acid co-oxidation with peroxidase/hydrogen peroxide. Further evidence for radical intermediates. *Biochem Pharmacol* 1989; **38**: 1209–1216.
20. Abe S, Kirima K, Tsuchiya K *et al.* The reaction rate of edaravone (3-methyl-1-phenyl-2-pyrazolin-5-one (MCI-186)) with hydroxyl radical. *Chem Pharm Bull* 2004; **52**: 186–191.
21. Eiserich JP, Hristova M, Cross CE *et al.* Formation of nitric oxide-derived inflammatory oxidants by myeloperoxidase in neutrophils. *Nature* 1998; **391**: 393–397.

Neurogenetics (2008) 9:61–63
DOI 10.1007/s10048-007-0110-4

SHORT COMMUNICATION

Myotonic dystrophy type 2 in Japan: ancestral origin distinct from Caucasian families

Tsukasa Saito · Yoshinobu Amakusa · Takashi Kimura · Osamu Yahara · Hitoshi Aizawa · Yoshio Ikeda · John W. Day · Laura P. W. Ranum · Kinji Ohno · Tohru Matsuura

Received: 10 September 2007 / Accepted: 7 November 2007 / Published online: 5 December 2007

Abstract Myotonic dystrophy type 2 (DM2) is caused by expansion of a tetranucleotide CCTG repeat in intron 1 of the *ZNF9* gene on chromosome 3q21. All studied DM2 mutations have been reported in Caucasians and share an identical haplotype, suggesting a common founder. We identified a Japanese patient with DM2 and showed that the affected haplotype is distinct from the previously identified DM2 haplotype shared among Caucasians. These data strongly suggest that DM2 expansion mutations originate from separate founders in Europe and Japan and are more widely distributed than previously recognized.

Keywords Myotonic dystrophy type 2 · CCTG tetranucleotide repeat expansion · Founder haplotype

Saito and Amakusa have contributed equally to the work.

Electronic supplementary material The online version of this article (doi:10.1007/s10048-007-0110-4) contains supplementary material, which is available to authorized users.

T. Saito · T. Kimura · O. Yahara
Department of Neurology, National Dohoku Hospital, Asahikawa, Japan

Y. Amakusa · K. Ohno · T. Matsuura (✉)
Division of Neurogenetics and Bioinformatics, Center for Neurological Diseases and Cancer, Nagoya University Graduate School of Medicine, Nagoya 466-8550, Japan
e-mail: tohrum@med.nagoya-u.ac.jp

T. Saito · H. Aizawa
Division of Neurology, Department of Internal Medicine, Asahikawa Medical College, Asahikawa, Japan

Y. Ikeda · J. W. Day · L. P. W. Ranum
Institute of Human Genetics, University of Minnesota, Minneapolis, MN, USA

Y. Ikeda · L. P. W. Ranum
Department of Genetics, Cell Biology, and Development, University of Minnesota, Minneapolis, MN, USA

J. W. Day
Department of Neurology, University of Minnesota, Minneapolis, MN, USA

Introduction

Myotonic dystrophy type 2 (DM2) is an autosomal dominant, myotonic multisystemic disorder caused by the expansion of a tetranucleotide CCTG repeat in intron 1 of the zinc finger protein 9 (*ZNF9*) gene on chromosome 3q21 [1]. The size of expanded alleles is extremely variable, ranging from 75 to 11,000 repeats, with a very large mean of 5,000 CCTG repeats. Because of this unprecedented size and somatic heterogeneity, molecular diagnosis of DM2 is complicated. DM2 is also clinically variable, described as proximal myotonic myopathy [2], proximal myotonic dystrophy [3], or "myotonic dystrophy with no CTG expansion" [4]. Further studies suggested that all genetically confirmed DM2 patients arose from a single ancestral origin [5, 6]. No DM2 mutation, to date, has been identified in sub-Saharan or East-Asian populations [7]. Herein, we report the first Japanese family with a DM2 mutation.

Case report

A 59-year-old Japanese woman was admitted to our hospital for weakness of all four limbs that had progressed

slowly for more than 12 years. There was no complaint of muscle pain or stiffness. At age 47, she developed type 2 diabetes mellitus. At age 52, she had a right posterior subcapsular cataract extracted. There was no known consanguinity or genetic admixture with other ethnicities in her family. Her father and mother had no history of muscle weakness before having died at ages 67 and 72 years, respectively. There was a history of undiagnosed muscle disease in her brother and sister, but they were unavailable for examination. Her two children were asymptomatic.

Neurologically, this patient had normal language, speech, and cognition on routine clinical evaluation. She showed mild facial weakness and temporal wasting as well as weakness and atrophy of sternocleidomastoid muscles. Motor examination revealed predominantly proximal muscle weakness and atrophy in all limbs. Grip myotonia was present, but percussion myotonia was not elicitable. Tendon reflexes were present, but hypoactive and sensation was intact. Serum creatine kinase was 99 IU/l (normal range, 45–163 IU/l), and serum IgG level was slightly decreased to 828 mg/dl (normal range, 870–1,700 mg/dl). Electrocardiogram revealed complete right bundle branch block, and Holter monitoring detected premature ventricular contractions. Electromyography showed small motor unit potentials with early recruitment and myotonic discharges in all muscles examined. Nerve conduction studies were normal. Muscle computed tomography revealed diffuse muscle atrophy in the trunk and proximally in all limbs, whereas forearm and distal leg muscles were well preserved (Supplementary Figs. 2 and 3). T2-weighted brain magnetic resonance imaging demonstrated diffuse periventricular white matter hyperintensities without significant cerebral atrophy. No CTG expansion in the *DMPK* gene associated with myotonic dystrophy type 1 (DM1) [8] was detected.

Materials and methods

Mutation analysis

Blood samples were obtained from the patient and her family members with informed consent approved by the institutional review boards of the National Dohoku Hospital and the Nagoya University Graduate School of Medicine for human research. High molecular weight genomic DNA was extracted by a standard procedure. Polymerase chain reaction (PCR) products across the DM2 repeat (marker CL3N58) in the first intron of the *ZNF9* [1] were analyzed by capillary electrophoresis using an automated DNA sequencer (ABI 310A Genetic Analyzer, Applied Biosystems). For detection of the DM2 CCTG expansion, Southern blot analysis and the repeat-primed PCR assay using an oligonucleotide primed within the DM2 CCTG repeat were performed as described elsewhere [1, 9, 10].

Haplotype analysis

To investigate the ancestral origin of Japanese DM2, we performed a haplotype analysis of our patient's family. We genotyped available family members (the patient, her spouse, and two children) for the previously described microsatellite markers: CL3N83; CL3N95; CL3N96; CL3N59; C3N116; CL3N117; CL3N118; CL3N119 [6] and a single nucleotide polymorphism (SNP): rs1871922, which is identical to TSC873597 in the report by Bachinski et al. [5]. We also analyzed three unrelated Caucasian DM2 DNA samples sharing the identical core haplotype as controls [6]. PCR products for all microsatellite markers were analyzed, and the SNP genotyping was performed by PCR amplification followed by restriction enzyme digestion (*Hae*III). The data were compared to the consensus Caucasian haplotypes reported in the previous report [6].

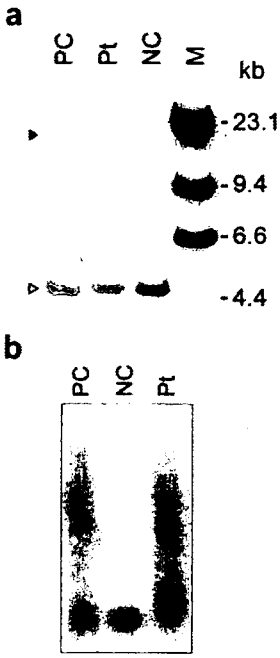

c

Location (kb)	Marker	Our pedigree	Caucasian haplotype B	Caucasian haplotype A	Caucasian haplotype C
273	CL3N83	191	189	195	185
241	CL3N95	224	222	222	212
240	CL3N96	159	159	159	157
119	CL3N59	129	149	149	141
0	DM2 repeat	exp.	exp.	exp.	exp.
11	rs1871922	A	C	C	C
74	CL3N116	222	222	222	222
103	CL3N117	239	235	235	235
127	CL3N118	227	221	221	221
216	CL3N119	220	234	230	230

Fig. 1 **a** Southern blot analysis of myotonic dystrophy type 2 (DM2). A *closed arrowhead* points to expanded alleles in DM2. *M* λDNA/*Hind* III marker, *NC* normal control, *Pt* our patient showing an 18.1-kb expanded allele as well as a normal allele, *PC* a Caucasian positive control with a DM2 expansion (17.5 kb). **b** Repeat-primed PCR analysis. Expanded CCTG repeats are detected as a continuous characteristic ladder in the patient (*Pt*) and positive control (*PC*) lanes, the size of which exceeds the range in the normal control (*NC*). **c** Comparison of DM2-affected haplotypes between Japanese and Caucasian DM2 families. Genotypes shared among Caucasian haplotypes are *shaded*. The distance of each marker from the DM2 CCTG repeat expansion (*exp*) is denoted on the *left*

Results

Mutation analysis

PCR amplification of the DM2 repeat detected a single normal allele at 228 bp. To determine if this patient also had a disease allele too large to be amplified by PCR, Southern analysis was performed and showed an expanded DM2-mutant allele of 18.1 kb, corresponding to approximately 3,400 CCTG repeats, as well as a normal allele of 4.5 kb (Fig. 1a). The repeat-primed PCR assay also showed a smear PCR product, confirming the presence of DM2 CCTG expansion (Fig. 1b).

Haplotype analysis

As shown in Fig. 1c, we found that this patient has an expansion-associated haplotype distinct from that commonly found in Caucasian DM2 patients [5, 6], indicating a different ancestral origin. Although a short common haplotype, less than 130 kb, between CL3N59 and rs1871922, is still possible, a telomeric recombination between the mutation and the SNP (11 kb telomeric of the mutation) is unlikely.

Discussion

Consistent with the typical DM2 phenotype [7, 10, 11], our patient clinically showed a combination of adult-onset proximal muscle weakness and myotonia. To our knowledge, this is the first DM2 patient identified from an East-Asian population [7]. Although DM2 mutations were reported in non-European populations including Morocco, Algeria, Lebanon, Afghanistan, and Sri Lanka [7, 11], all reported DM2 patients were considered to originate from a single common founder because they shared an identical haplotype [5, 6]. Our data have implications for molecular genetic diagnostics and counseling of East-Asian patients with the DM clinical phenotype and their families, as well as providing insight into the evolution of this complex disease. Physicians and genetic counselors should be aware that DM2 exists in non-Caucasian populations. Further epidemiologic studies, especially collection of additional non-Caucasian DM2 patients, will be of interest. It will also be of value to determine whether DM2 patients of different ethnic backgrounds originated from separate founders and whether they have unique clinical features and differences in genetic instability.

Acknowledgements We are grateful to our patient and her family for participating. This study was supported by research Grants-in-Aid from the Ministry of Health, Labor and Welfare of Japan (17A-1, 17A-8, 17A-10) (K.O., T.K.), Takeda Science Foundation, Japan (K.O., T.M.), Sankyo Foundation of Life Science, Kato Memorial Trust for Nanbyo Research, Nagono Medical Foundation, Nitto Foundation, Japan Brain Foundation, Japan (T.M.).

The experiments performed comply with current legislation in Japan.

References

1. Liquori CL, Ricker K, Moseley ML, Jacobsen JF, Kress W, Naylor SL, Day JW, Ranum LP (2001) Myotonic dystrophy type 2 caused by a CCTG expansion in intron 1 of ZNF9. Science 293:864–867
2. Ricker K, Koch MC, Lehmann-Horn F, Pongratz D, Otto M, Heine R, Moxley RT 3rd (1994) Proximal myotonic myopathy: a new dominant disorder with myotonia, muscle weakness, and cataracts. Neurology 44:1448–1452
3. Udd B, Krahe R, Wallgren-Petterson C, Falck B, Kalimo H (1997) Proximal myotonic dystrophy: a family with autosomal dominant muscular dystrophy, cataracts, hearing loss and hypogonadism: heterogeneity of proximal myotonic syndromes? Neuromuscul Disord 7:217–228
4. Thornton CA, Griggs RC, Moxley RT (1994) Myotonic dystrophy with no trinucleotide repeat expansion. Ann Neurol 35:269–272
5. Bachinski LL, Udd B, Meola G, Sansone V, Bassez G, Eymard B, Thornton CA, Moxley RT, Harper PS, Rogers MT, Jurkart-Rott K, Lehmann-Horn F, Wieser T, Gamez J, Navarro C, Bottani A, Kohler A, Shriver MD, Sallinen R, Wessman M, Zhang S, Wright FA, Krahe R (2003) Confirmation of type 2 myotonic dystrophy $(CCTG)_n$ expansion mutation in patients with proximal myotonic myopathy/proximal myotonic dystrophy of different European origins: a single shared haplotype indicates an ancestral founder effect. Am J Hum Genet 73:835–848
6. Liquori CL, Ikeda Y, Weatherspoon M, Ricker K, Schoser BGH, Dalton JC, Day JW, Ranum LPW (2003) Myotonic dystrophy type 2: human founder haplotype and evolutionary conservation of the repeat tract. Am J Hum Genet 73:849–862
7. Udd B, Meola G, Krahe R, Thornton C, Ranum LPW, Bassez G, Kress W, Schoser B, Moxley R (2006) 140th ENMC International Workshop: myotonic dystrophy DM2/PROMM and other myotonic dystrophies with guidelines on management. Neuromuscul Disord 16:403–413
8. Brook JD, McCurrach ME, Harley HG, Buckler AJ, Church D, Aburatani H, Hunter K, Stanton VP, Thirion JP, Hudson T, Sohn R, Zemelman B, Snell RG, Rundle SA, Crow S, Davies J, Shelbourne P, Buxton J, Jones C, Juvonen V, Johnson K, Harper PS, Shaw DJ, Housman DE (1992) Molecular basis of myotonic dystrophy: expansion of a trinucleotide (CTG) repeat at the 3′ end of a transcript encoding a protein kinase family member. Cell 168:799–808 (erratum 69:385)
9. Furuya H, Yamada T, Ikezoe K, Ohyagi Y, Fukumaki Y, Fujii N (2006) An improved method for Southern DNA and Northern RNA blotting using a Mupid-2 mini-gel electrophoresis unit. J Biochem Biophys Methods 68:139–143
10. Day JD, Ricker K, Jacobsen JF, Rasmussen LJ, Dick KA, Kress W, Schneider C, Koch MC, Beilman GJ, Harrison AR, Dalton JC, Ranum LPW (2003) Myotonic dystrophy type 2: molecular, diagnostic and clinical spectrum. Neurology 60:657–664
11. Udd B, Meola G, Krahe R, Thornton C, Ranum L, Day J, Bassez G, Ricker K (2003) Report of the 115th ENMC Workshop: DM2/PROMM and other myotonic dystrophies: 3rd workshop. Neuromuscul Disord 13:589–596

NEUROLOGY

Evaluation of corticospinal tracts in ALS with diffusion tensor MRI and brainstem stimulation

N. K. Iwata, S. Aoki, S. Okabe, N. Arai, Y. Terao, S. Kwak, O. Abe, I. Kanazawa, S. Tsuji and Y. Ugawa

Neurology 2008;70;528-532
DOI: 10.1212/01.wnl.0000299186.72374.19

Evaluation of corticospinal tracts in ALS with diffusion tensor MRI and brainstem stimulation

N.K. Iwata, MD, PhD
S. Aoki, MD, PhD
S. Okabe, MD, PhD
N. Arai, MD, PhD
Y. Terao, MD, PhD
S. Kwak, MD, PhD
O. Abe, MD, PhD
I. Kanazawa, MD, PhD
S. Tsuji, MD, PhD
Y. Ugawa, MD, PhD

Address correspondence and reprint requests to Dr. Nobue K. Iwata, Human Motor Control Section, Medical Neurology Branch, National Institute of Neurological Disorders and Stroke, National Institutes of Health, Building 10, Room 5N226, 10 Center Drive, Bethesda, MD 20892-1428
iwatan@ninds.nih.gov

ABSTRACT

Objective: To assess corticospinal tract involvement in patients with amyotrophic lateral sclerosis (ALS) by correlating diffusion tensor imaging (DTI) measures with intra- and extracranial central motor conduction time (CMCT) and clinical features of the patients.

Methods: We investigated 31 patients with ALS and 31 normal volunteers by DTI and measured fractional anisotropy (FA) within the corticospinal tracts and in the extramotor white matter. We measured CMCT for the first dorsal interosseous muscle and segmented it into cortical-brainstem (CTX-BS CT) and brainstem-cervical root (BS-CV CT) conduction times by magnetic brainstem stimulation at the foramen magnum level. Clinical status of each patient was evaluated with the ALS Functional Rating Scale-Revised (ALSFRS-R) and upper motor neuron (UMN) score devised for this study.

Results: We found a significant decrease of mean FA in all regions of the corticospinal tracts in patients with ALS as compared with controls. We found that FA along the corticospinal tract decreased significantly with higher UMN scores. There was no significant correlation between FA and ALSFRS-R, to which both upper and lower motoneuron involvements contribute. FA showed a significant correlation with the intracranial part of the central motor conduction (CTX-BS CT) but not with the extracranial conduction time.

Conclusions: Fractional anisotropy reflects functional abnormality of intracranial corticospinal tracts and can be used for objective evaluation of upper motor neuron impairment in amyotrophic lateral sclerosis. ***Neurology*** 2008;70:528-532

GLOSSARY

ALS = amyotrophic lateral sclerosis; **ALSFRS-R** = ALS Functional Rating Scale-Revised; **BS-CV CT** = brainstem-cervical root conduction time; **CMCT** = central motor conduction time; **CTX-BS CT** = cortical-brainstem conduction time; **FA** = fractional anisotropy; **FDI** = first dorsal interosseous; **LMN** = lower motor neuron; **ROI** = region of interest; **UMN** = upper motor neuron.

Amyotrophic lateral sclerosis (ALS) is clinically diagnosed by lower motor neuron (LMN) signs of limb and bulbar muscles associated with upper motor neuron (UMN) signs. Subclinical LMN involvement is detectable by needle electromyographic findings of denervation, which are incorporated in revised El Escorial criteria.[1] UMN involvement can be evaluated by physiologic measures or neuroimaging techniques,[2] although these have not been sufficiently well established to be incorporated into diagnostic criteria. Diffusion tensor MRI visualizes the overall orientation of the fiber tracts and their integrity in the white matter by measuring anisotropic water diffusion.[3] Decreased fractional anisotropy (FA) along the corticospinal tract has recently been reported in patients with ALS.[4,5] However, the pathophysiology of such reduced FA remains unclear. The present

From the Department of Neurology, Division of Neuroscience (N.K.I., S.O., N.A., Y.T., S.K., I.K., S.T., Y.U.), and Department of Radiology and Bioengineering (S.A., O.A.), Graduate School of Medicine, University of Tokyo; National Institute of Neuroscience (I.K.), National Center of Neurology and Psychiatry, Tokyo, Japan; and Human Motor Control Section (N.K.I.), Medical Neurology Branch, National Institute of Neurological Disorders and Stroke, National Institutes of Health, Bethesda, MD.

Supported by Research Project Grant-in-Aid for Scientific Research 16500194 from the Ministry of Education, Culture, Sports, Science, and Technology of Japan; Research Grant 15B-2 for Nervous and Mental Disorders from the Ministry of Health, Labor, and Welfare of Japan; a grant from the Committee of the Study of Human Exposure to EMF; the Ministry of Internal Affairs and Communications; grants from the Life Science Foundation of Japan and the Association of Radio-industry and Business; and the Nakabayashi Trust for ALS Research.

Disclosure: The authors report no conflicts of interest.

investigation was undertaken with the intent of clarifying the mechanism for reduced FA in ALS by studying correlations of the FA value with central motor conduction time segmented into intracranial and extracranial conduction times using brainstem stimulation.

METHODS Subjects. We recruited 31 patients with ALS and 31 age-matched normal subjects (ALS 60.7 ± 12.9 years, normal 57.1 ± 13.0 years, $p = 0.166$). The Ethical Review Committee of the University of Tokyo approved this study. All subjects gave their written informed consent to participate in the study. All patients were enrolled if they met definite, probable, or possible categories of revised El Escorial criteria.[1] The degree of abnormality was quantified using the ALS Functional Rating Scale-Revised (ALSFRS-R). The UMN score was designed to assess UMN impairment. The following neurologic signs were rated on a 0 to 2 scale according to their severity (0 = absent or normal, 1 = moderately impaired, and 2 = greatly impaired): jaw jerk, other pathologic reflexes of the cranial regions, overactive tendon reflexes in upper limbs, overactive finger flexor reflexes, overactive tendon reflexes in lower limbs, pathologic reflexes in lower limbs, spasticity, and presence of clonus. The scale generates a score from 0 to 16.

Transcranial magnetic stimulation of corticospinal pathways. Central motor conduction time (CMCT) was measured with methods described previously,[6] recorded from the first dorsal interosseous (FDI) muscles. A round coil was used for motor cortical and spinal motor root stimulation, and a double cone coil was used for brainstem stimulation. CMCT (motor-evoked potential latency difference between motor cortical and cervical root simulation), cortical-brainstem conduction time (CTX-BS CT, latency difference between motor cortical and brainstem stimulation), and brainstem-cervical root conduction time (BS-CV CT, latency difference between brainstem and cervical root stimulation) were calculated and evaluated by neurophysiologists blinded to MRI results.

Diffusion tensor MRI scanning protocol. Diffusion tensor images were acquired with 1.5-tesla Signa Horizon LX MRI system (GE Medical Systems), using single-shot spin-echo echoplanar sequences (repeat time 6,000 msec, echo time 78 msec, field of view 24 cm, NEX 4, 128 × 128-pixel matrix, diffusion gradients [*b*-value of 1,000 sec/mm^2], 3-mm slice thickness). Diffusion properties were measured along 13 noncollinear directions. FA was measured using a region-of-interest (ROI) method. Elliptical ROIs were placed along bilateral corticospinal tracts (corona radiata, internal capsule, cerebral peduncle, basis pontis, and medulla oblongata) and extramotor white matters (genu and splenium of the corpus callosum, superior, middle, and inferior cerebellar peduncle, and cerebellar white matter) on FA maps by one author blinded to subject clinical status, based on empirical anatomic knowledge and reference to pertinent literature.

Statistical analyses. We used a two-way analysis of variance (ANOVA) (factors of subject group and region). We used Scheffe analysis as post hoc multiple comparisons (significance level 0.05). Linear regression analyses were applied for all correlations (significance level 0.05) using StatView software (version 5; SAS Institute). Because FA is reported to decline with advancing age,[7] correlations between FA and clinical or physiologic measures are examined by using ratio of FA at each ROI to that of the splenium of the corpus callosum, to compensate for interindividual variability of absolute FA values. In evaluation of correlations between FA and CMCT as well as CTX-BS CT and BS-CV CT, we used all FA values and compatible physiologic measures, such as a FA on one side and a physiologic measure for the contralateral FDI. When a correlation between anisotropy data and ALSFRS-R or UMN score was analyzed, we averaged values from right and left sides to provide a single mean FA at a site for each individual.

Figure 1 Individual plots of fractional anisotropy (FA) at each region of interest (ROI) for patients with amyotrophic lateral sclerosis (filled circles) and controls (open circles) (mean ± SD)

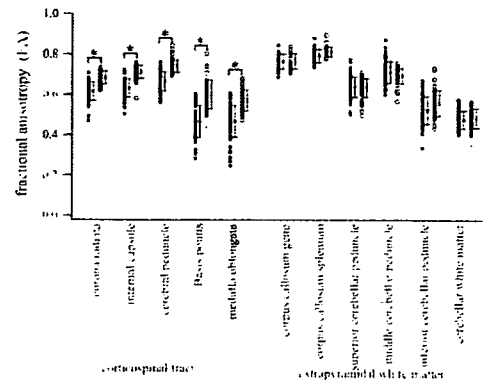

RESULTS Fractional anisotropy. Individual plots of FA at each ROI for patients with ALS and controls are shown in figure 1. Two-way ANOVA showed an effect of the subject group (patient and control) and region (effect of subject group: $F = 205.763$, $p < 0.0001$; effect of region: $F = 395.421$, $p < 0.0001$). It also showed an interaction between the subject group and region ($F = 25.457$, $p < 0.0001$). Post hoc analyses showed that the mean FA was lower in patients with ALS than in controls in all ROI within the corticospinal tracts (the corona radiata, posterior limb of the internal capsule, cerebral peduncle, basis pontis, pyramid of the medulla oblongata) ($p < 0.0005$). No significant differences were found within extramotor white matter. FA decreased significantly with higher UMN scores at corona radiata, internal capsule, and pyramids of medulla oblongata. No correlation was apparent between UMN scores and FA in extramotor white matter. FA showed no significant correlation with ALSFRS-R in any

Table 1 Correlation between fractional anisotropy (FA) and clinical/physiologic measures

	Correlation between FA and clinical measures		Correlation between FA and physiologic measures		
Site	ALSFRS-R	UMN score	CMCT	CTX-BS CT	BS-CV CT
FA of corticospinal tract					
Corona radiata	0.070 (0.707)	0.397 (0.027*)	0.432 (0.004*)	0.409 (0.020*)	0.236 (0.201)
Internal capsule	0.292 (0.111)	0.440 (0.013*)	0.547 (<0.0001*)	0.535 (0.002*)	0.249 (0.176)
Cerebral peduncle	0.307 (0.093)	0.173 (0.353)	0.284 (0.065)	0.178 (0.330)	0.264 (0.152)
Basis pontis	0.037 (0.843)	0.210 (0.258)	0.306 (0.046*)	0.378 (0.033*)	0.073 (0.696)
Medulla oblongata	0.215 (0.245)	0.436 (0.014*)	0.408 (0.007*)	0.349 (0.051)	0.239 (0.195)
FA of extracorticospinal tract					
Corpus callosum genu	0.136 (0.465)	0.147 (0.429)	0.072 (0.751)	0.085 (0.763)	0.093 (0.741)
Superior cerebellar peduncle	0.120 (0.520)	0.071 (0.704)	0.213 (0.171)	0.083 (0.652)	0.106 (0.571)
Middle cerebellar peduncle	0.105 (0.574)	0.035 (0.853)	0.249 (0.108)	0.183 (0.315)	0.173 (0.353)
Inferior cerebellar peduncle	0.105 (0.575)	0.044 (0.814)	0.005 (0.974)	0.064 (0.727)	0.037 (0.843)
Cerebellar white matter	0.321 (0.078)	0.100 (0.591)	0.061 (0.698)	0.092 (0.616)	0.149 (0.425)

Correlation coefficient and the respective *p* value are shown.
*Significant.
ALSFRS-R = ALS Functional Rating Scale-Revised; BS-CV CT = brainstem-cervical root conduction time; CMCT = central motor conduction time; CTX-BS CT = cortical-brainstem conduction time; UMN = upper motor neuron.

ROI (table 1).

Transcranial magnetic stimulation of corticospinal pathways. We examined 47 limbs of 25 patients. In 16 limbs of 10 patients, no responses were obtained with motor cortical, brainstem, or motor root stimulation. The averaged ALSFRS-R of these patients was 29.7 ± 11.7, which was worse than that of the rest of the patients (36.7 ± 8.2, $p < 0.05$). There was no difference in the averaged UMN scores between the two patient groups (6.3 ± 3.8 and 6.2 ± 4.1, $p > 0.05$). Theoretically, unobtainable responses are attributable to cortical inexcitability resulting from motor cortical cell loss, severe peripheral involvement, or a combination of both. However, in the patients studied here, based on the above results of correlations, we can infer that dysfunction of LMN contributes more than that of the UMN to the lack of responses. These absent responses were excluded from the following correlation analyses because there were no measurable latencies.

In all, we obtained 43 CMCTs and 31 CTX-BS CTs as well as BS-CV CTs. The averaged CMCT of FDI of the patients was 8.5 ± 3.4 msec (the average ± SD of the normal subjects at our facility was 7.0 ± 0.4 msec). Seventeen of 43 CMCTs were abnormally delayed (above the average + 2SD of the normal values). The average of CTX-BS CTs from the patients was 4.4 ± 3.0 msec (the normal average was 3.3 ± 0.3 msec). Twelve of 31 CTX-BS CTs were delayed. The average of BS-CV CTs of the patients was 4.3 ± 2.9 (the normal average was 3.7 ± 0.5), and 12 of 31 BS-CV CTs were abnormally prolonged. We found overall abnormal results including absent responses to either cortical or root stimulation, and delayed responses, in 44.7% of all the limbs studied. Delayed CMCT, CTX-BS CT, and BS-CV CT were found in 39.5%, 38.7%, and 38.7% of recorded responses. CMCT and CTX-BS CT correlated significantly with both ALSFRS-R and UMN scores, but BS-CV CT correlated only with ALSFRS-R (table 2).

Table 2 Correlations between central motor conduction times and clinical indices

Measures	Correlation	*p* Value
CMCT vs		
ALSFRS-R	0.482	0.0011*
UMN score	0.598	<0.0001*
CTX-BS CT vs		
ALSFRS-R	0.457	0.0098*
UMN score	0.595	0.0004*
BS-CV CT vs		
ALSFRS-R	0.559	0.0011*
UMN score	0.234	0.2048

*Significant.
CMCT = central motor conduction time; ALSFRS-R = ALS Functional Rating Scale-Revised; BS-CV CT = brainstem-cervical root conduction time; CTX-BS CT = cortical-brainstem conduction time; UMN = upper motor neuron.

Figure 2 Regression plots of fractional anisotropy at the internal capsule as a function of cortical-brainstem conduction time (CTX-BS CT) (A) and brainstem-cervical root conduction time (BS-CV CT) (B)

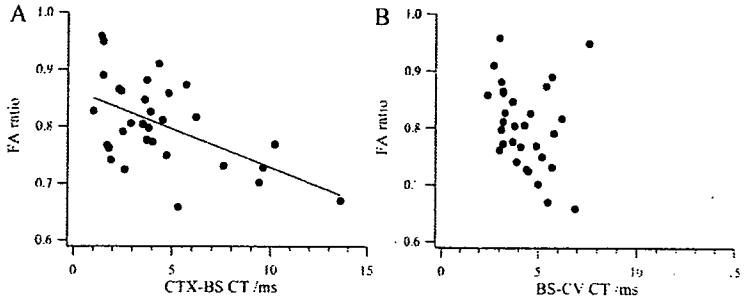

Correlation was only apparent between FA and cortical-brainstem conduction time ($|r| = 0.535, p = 0.002$). No correlation was observed between FA and the extracranial conduction time (brainstem-cervical root conduction time) ($|r| = 0.249, p = 0.176$).

Correlation between FA and CMCTs. FAs at most regions along the corticospinal tract decreased significantly with delayed CMCT and CTX-BS CT (table 1, figure 2A). However, BS-CV CT did not correlate with FA in any ROI (figure 2B). No significant correlation was found between FA of extramotor regions and CMCT or CTX-BS CT.

DISCUSSION In ALS, we have demonstrated reduced FA restricted to the corticospinal tracts. We also found that FA along the corticospinal tract decreased with higher UMN scores or delayed CTX-BS CT. The brainstem stimulation is considered to differentiate the CMCT delay due to an intracranial lesion from that due to an extracranial spinal lesion.[8] The CTX-BS CT must purely reflect UMN function, whereas the BS-CV CT must mostly reflect LMN function, and CMCT both LMN and UMN functions. Based on this theory, our present results suggest that FA measurement can evaluate UMN function in patients.

We showed that CTX-BS CT, but not BS-CV CT, delayed significantly with decreased FA at sites of the corticospinal tracts other than the cerebral peduncle where CSF has a greater partial volume effect on images. Decreased FA suggests tract degeneration that engenders the loss of organized coherent structures. FA changes are explainable by both intracellular water diffusion changes and extracellular matrix changes. Previous histopathologic studies of ALS suggest that the former corresponds to degeneration of the corticospinal tract axon itself with associated astrocytosis and accumulation of axonal spheroids, whereas the latter corresponds to extracellular matrix expansion and astrocytosis within interaxonal spaces. Both processes can cause reduced anisotropy of water diffusion. Meanwhile, slowing of the conduction time is considered to result from the loss of larger and faster conducting neurons and reduction of functioning rapidly conducting axons following corticospinal cell loss.[9] From animal experiments, the magnitude of latency delay by failed firing attributable to functioning fiber loss is estimated to be a few milliseconds at maximum from the cortex to cervical spinal cord. A striking increase of the conduction time in excess of this range would suggest slowing of conduction itself, which might be attributable to conduction through slowly conducting fibers due to degeneration of rapidly conducting fibers, or secondary demyelination when cortical neuronal loss is severe. These inferences are supported by white matter histopathology of the corticospinal tract: Myelin loss is commonly observed, especially in advanced patients, and the severity of that loss is generally related to neuronal loss of the motor cortex.[10] With the finding that the FA along the corticospinal tract decreased with intracranial motor conduction delay in ALS, we can infer that impaired axonal function, rather than extracellular factors, mainly contributes to the reduced FA. Demyelination secondary to motor axonal loss may add water diffusion changes in patients with excessive delayed motor conduction. This idea is consistent with the current view of determinants of anisotropy that the primary contributor is axonal membrane function, whereas other microstructures such as the myelin sheath, the neurofibrils (microtubules, neurofilaments), and axonal transport can play a secondary modulating role.[11] For more precise elucidation on potential determinants of anisotropic changes in ALS, thorough comparative studies of diffusion tensor imaging and postmortem specimens are necessary.

We demonstrated a significant correlation of FA with other clinical or physiologic indices. Potential applications of this method for patients with ALS include its use as an objective marker in following the natural course of the disease or modified course in therapeutic trials, or detecting a mild lesion of the corticospinal tracts at early stages.

ACKNOWLEDGMENT

The authors thank Dr. Peter T. Lin for helpful comments.

Received September 21, 2005. Accepted in final form August 8, 2007.

REFERENCES

1. Brooks BR, Miller RG, Swash M, Munsat TL. World Federation of Neurology Research Group on Motor Neuron Diseases. El Escorial revisited: revised criteria for the diagnosis of amyotrophic lateral sclerosis.

Amyotroph Lat Scler Other Motor Neuron Disord 2000;1:293–299.
2. Kaufmann P, Pullman SL, Shungu DC, et al. Objective tests for upper motor neuron involvement in amyotrophic lateral sclerosis (ALS). Neurology 2004;62:1753–1757.
3. Basser PJ, Pierpaoli C. Microstructural and physiological features of tissues elucidated by quantitative-diffusion-tensor MRI. J Magn Reson B 1996;111:209–219.
4. Ellis CM, Simmons A, Jones DK, et al. Diffusion tensor MRI assesses corticospinal tract damage in ALS. Neurology 1999;53:1051–1058.
5. Sach M, Winkler G, Glauche V, et al. Diffusion tensor MRI of early upper motor neuron involvement in amyotrophic lateral sclerosis. Brain 2004;127:340–350.
6. Ugawa Y, Uesaka Y, Terao Y, Hanajima R, Kanazawa I. Magnetic stimulation of corticospinal pathways at the foramen magnum level in humans. Ann Neurol 1994;36:618–624.
7. Abe O, Aoki S, Hayashi N, et al. Normal aging in the central nervous system: quantitative MR diffusion-tensor analysis. Neurobiol Aging 2002;23:433–441.
8. Ugawa Y, Uesaka Y, Terao Y, et al. Clinical utility of magnetic corticospinal tract stimulation at the foramen magnum level. Electroencephalogr Clin Neurophysiol 1996;101:247–254.
9. Thompson PD, Day BL, Rothwell JC, et al. The interpretation of electromyographic responses to electrical stimulation of the motor cortex in diseases of the upper motor neurone. J Neurol Sci 1987;80:91–110.
10. Lowe JS, Leigh N. Disorders of movement and system degeneration. In: Graham DJ, Lantos PL, eds. Greenfield's neuropathology, Vol. 2, 7th ed. London: Arnold; 2002: 325–430.
11. Beaulieu C. The basis of anisotropic water diffusion in the nervous system: a technical review. NMR Biomed 2002;15:435–455.

Evaluation of corticospinal tracts in ALS with diffusion tensor MRI and brainstem stimulation

N. K. Iwata, S. Aoki, S. Okabe, N. Arai, Y. Terao, S. Kwak, O. Abe, I. Kanazawa, S. Tsuji and Y. Ugawa

Neurology 2008;70;528-532
DOI: 10.1212/01.wnl.0000299186.72374.19

The Receiving editor; Dr. Nobuyuki Nukina

Determination of editors at the novel A-to-I editing positions

Yoshinori Nishimoto[a,b,*], Takenari Yamashita[a,*], Takuto Hideyama[a], Shoji Tsuji[a], Norihiro Suzuki[b], Shin Kwak[a]

[a] Department of Neurology, Graduate School of Medicine, University of Tokyo, 7-3-1 Hongo, Bunkyo-ku, Tokyo 113-8655, Japan

[b] Department of Neurology, Graduate School of Medicine, Keio University, 35 Shinanomachi, Shinjuku-ku, Tokyo 160-8582, Japan

*These authors equally contributed to this study.

Corresponding author: Shin Kwak, Department of Neurology, Graduate School of Medicine, University of Tokyo, 7-3-1 Hongo, Bunkyo-ku, Tokyo 113-8655, Japan, kwak-tky@umin.ac.jp

This manuscript consists of 4,332 words in 17 pages, including four figures and no table.

The supplementary file is also attached.

ABSTRACT

A-to-I RNA editing modifies a variety of biologically important mRNAs, and is specifically catalyzed by either adenosine deaminase acting on RNA type 1 (ADAR1) or type 2 (ADAR2) in mammals including human. Recently several novel A-to-I editing sites were identified in mRNAs abundantly expressed in mammalian organs by means of computational genomic analysis, but which enzyme catalyzes these editing sites has not been determined. Using RNA interference knockdowns, we found that cytoplasmic fragile X mental retardation protein interacting protein 2 (CYFIP2) mRNA had an ADAR2-mediated editing position and bladder cancer associated protein (BLCAP) mRNA had an ADAR1-mediated editing position. In addition, we found that ADAR2 forms complex with mRNAs with ADAR2-mediated editing positions including GluR2, kv1.1 and CYFIP2 mRNAs, particularly when the editing sites were edited in human cerebellum by means of immunoprecipitation method. CYFIP2 mRNA was ubiquitously expressed in human tissues with variable extents of K/E site-editing. Because ADAR2 underactivity may be a causative molecular change of death of motor neurons in sporadic ALS, this newly identified ADAR2-mediated editing position may become a useful tool for ALS research.

Keywords:

RNA editing, adenosine deaminase acting on RNA (ADAR), immunoprecipitation(IP), RNA interference (RNAi), cytoplasmic fragile X mental retardation protein interacting protein 2 (CYFIP2), bladder cancer associated protein (BLCAP)

1. INTRODUCTION

Adenosine deaminases acting on RNA (ADARs) catalyze A-to-I RNA editing in a wide range of organisms including human. Among three structurally related ADARs (Keegan et al., 2001; Bass, 2002; Maas et al., 2003), ADAR1 is indispensable for normal development (Wang et al., 2000) and ADAR2 plays a key role in the regulation of neuronal excitability in mice (Brusa et al., 1995; Higuchi et al., 2000), and presumably in the pathogenesis of sporadic amyotrophic lateral sclerosis (ALS) in humans, by specifically editing the Q/R site of GluR2, a subunit of the α-amino-3-hydroxy-5-methyl-4-isoxazolepropionic acid (AMPA) receptor (Takuma et al., 1999; Kawahara et al., 2004; Kwak & Kawahara, 2005). Extensive A-to-I conversion occurs in the large numbers of mRNAs (Burns et al., 1997; Higuchi et al., 2000; Wang et al., 2000; Bhalla et al., 2004), and studies using a computational genomic approach have recently demonstrated several novel A-to-I editing sites in mRNAs abundantly expressed in peripheral as well as neuronal tissues (Levanon, E.Y. et al., 2005). Using immunoprecipitation and the RNA interference (RNAi) knockdown system *in vitro*, we investigated whether the recently reported A-to-I editing sites in cytoplasmic fragile X mental retardation protein interacting protein 2 (CYFIP2), filamin A (FLNA), bladder cancer associated protein (BLCAP), and insulin-like growth factor binding protein 7 (IGFBP7) mRNAs (Levanon, E.Y. et al., 2005) are the substrates of ADAR1 or ADAR2 in humans. Furthermore, we also investigated whether these mRNAs in humans form complex with ADAR2 by means of ADAR2-immunoprecipitation method on nuclear extracts of human cerebellum.

2. Materials and methods

2.1. Isolation of RNA-protein complexes

The nuclear pellet was extracted from 6 g of frozen human cerebella. Briefly, after homogenizing the tissue in ten-volumes of cold 0.25 M sucrose in buffer A (Tris-saline-HCl buffer (pH7.5) containing 25 mM KCl, 5 mM $MgCl_2$ and 1 mM dithiothreitol), the nuclear pellet was obtained by centrifuging the P1-homogenate in 1.6 M sucrose in buffer A at 130,000×g for 1 h. The RNA-protein complex was isolated from the nuclear pellet according to previously described methods (Ohlson et al., 2005). Briefly, the nuclear pellet was sonicated in 8 ml of ice-cold buffer solution containing 0.1% sodium dodecylsulphate (SDS), 0.5% sodium deoxycholate, 0.5% Igepal CA-630 (Sigma Chemicals, St. Lois, MO) and 1mM ribonucleoside vanadyl complex (Sigma), and then treated with 800 units of DNase I (Sigma). The resultant solution was centrifuged at 10,000×g, 4°C for 20 min, and RNA-protein complexes were obtained in the supernatant. All studies were carried out in accordance with the Declaration of Helsinki and the Ethics Committee of the University of Tokyo has approved the experimental procedures used.

2.2. Immunoprecipitation of ADAR2-RNA complexes

Stock Sepharose G was prepared by suspending Protein G Sepharose 4 Fast Flow beads (swollen Sepharose G beads; GE healthcare Bioscience, Piscataway, NJ) treated with tRNA (1 mg/ml) and bovine serum albumin (1 mg/ml) in two volumes of phosphate buffered saline (PBS) containing 0.05% of NaN_3. First, after pre-clearing once with 50 µl of the untreated Sepharose G suspension in PBS, recombinant ADAR2a and FLAG-ADAR2a proteins which were prepared with TNT T7 Quick for PCR DNA